BIOCHEMISTRY
including biophysical chemistry & molecular biology

ARTICLE

pubs.acs.org/biochemistry

Structure and Activity of *Aspergillus nidulans* Copper Amine Oxidase

Aaron P. McGrath,[†,||] Suzanne M. Mithieux,[†] Charles A. Collyer,[†] Janny G. Bakhuis,[‡] Marco van den Berg,[‡] Arjen Sein,[‡] Andrea Heinz,[§] Christian Schmelzer,[§] Anthony S. Weiss,[†] and J. Mitchell Guss*[,†]

[†]School of Molecular Bioscience, University of Sydney, Sydney, NSW 2006, Australia

[‡]DSM Biotechnology Center, Delft, The Netherlands

[§]Institute of Pharmacy, Biosciences, Martin Luther University Halle-Wittenberg, Wolfgang-Langenbeck-Strasse 4, D-06120 Halle (Saale), Germany

ABSTRACT: *Aspergillus nidulans* amine oxidase (ANAO) has the unusual ability among the family of copper and trihydroxyphenylalanine quinone-containing amine oxidases of being able to oxidize the amine side chains of lysine residues in large peptides and proteins. We show here that in common with the related enzyme from the yeast *Pichia pastoris*, ANAO can promote the cross-linking of tropoelastin and oxidize the lysine residues in α-casein proteins and tropoelastin. The crystal structure of ANAO, the first for a fungal enzyme in this family, has been determined to a resolution of 2.4 Å. The enzyme is a dimer with the archetypal fold of a copper-containing amine oxidase. The active site is the most open of any of those of the structurally characterized enzymes in the family and provides a ready explanation for its lysine oxidase-like activity.

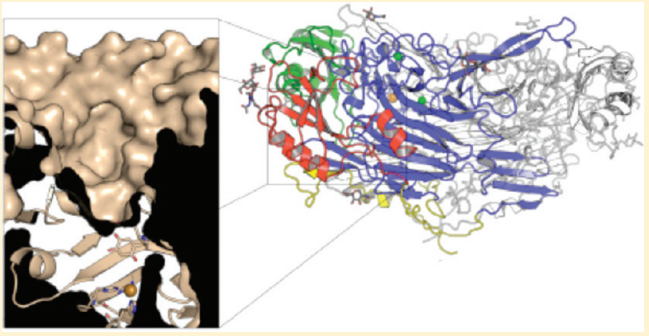

Amine oxidases are essential enzymes that catalyze the oxidation of a wide range of biogenic amines. They are utilized in a number of important biological processes ranging from the degradative metabolism of exogenous and endogenous amines (including neurotransmitters and mono-, di-, and polyamines) to the cross-linking of collagen and elastin by the oxidation of lysine peptides.[1] They catalyze the oxidative deamination of primary amines via the general reaction

$$R\text{-}CH_2\text{-}NH_3^+ + H_2O + O_2 \rightarrow RCHO + H_2O_2 + NH_4^+$$

Amine oxidases reduce dioxygen in the course of functionalizing amine substrates, and to facilitate this chemistry, they require organic cofactors as electron "sinks". Two distinct classes of amine oxidases exist: the flavin-containing monoamine oxidases (MAOs, EC 1.4.3.4) and the quinone- and copper-containing amine oxidases (CAOs, EC 1.4.3.6). Similarities between the two classes are apparent in the utilization of molecular oxygen as the electron acceptor, and mechanistically, catalysis similarly proceeds via H^+ abstraction as the initial C−H bond cleavage event.[1] In some instances, the two classes of amine oxidase have overlapping substrate profiles. However, despite these broad functional similarities, MAOs and CAOs differ in most other respects.

Two types of quinone cofactors exist in CAOs: 2,4,5-trihydroxyphenylalanine quinone (TPQ) and lysine tyrosyl quinone (LTQ). In both cases, quinone biogenesis proceeds via a novel self-processing reaction requiring only precursor protein, copper, and molecular oxygen.[2,3] Although both are copper-binding quinoenzymes, LTQ- and TPQ-containing CAOs share no overall sequence similarity. LTQ is found in lysyl oxidase (LOX[4]). The LOX gene encodes a 50 kDa proenzyme (Pro-LOX) that is secreted from cells and processed to the catalytically active 30 kDa LOX enzyme. LOX oxidizes peptidyl lysine side chains in immature collagen and elastin molecules.[5,6] The resultant aldehydic residues are highly reactive, spontaneously condensing with adjacent aldehydic or unmodified lysine residues initiating covalent cross-links. In this way, LOX facilitates the stabilization and insolubilization of fibrous collagen and elastin deposits in the extracellular mass in mammals.[7] LOX hence plays a critical role in the formation and repair of connective tissues. There is no three-dimensional structure available for a lysyl oxidase due in part to its insolubility making biophysical characterization difficult.

TPQ-containing CAOs (the abbreviation CAO will henceforth be restricted to the distinct TPQ-containing class of enzymes for the remainder of this paper), on the other hand, perform a variety of different roles between (and within) organisms. In general, CAOs possess ∼20−40% amino acid sequence identity and a high degree of structural homology, particularly in the immediate vicinity of the active site. Despite these similarities, a general role for CAOs in nature seems unlikely, and in many instances, individual roles for specific CAOs remain poorly defined. In the case of bacteria and yeasts, CAO activity allows growth in amine rich environments. In plants, CAOs are implicated

Received: April 13, 2011
Revised: May 20, 2011
Published: May 23, 2011

in processes such as wound healing and cell growth, with hydrogen peroxide produced during amine metabolism playing a possible role in the formation of suberin and lignin.[8] The functions of CAOs in higher organisms are less clear. In mammals, CAOs encompass a variety of roles, from the detoxification and inactivation of histamine and aliphatic diamines[9] to leukocyte adhesion at sites of inflammation and glucose uptake.[10]

X-ray crystal structures have been determined for CAOs from many organisms. Prior to this work, representative crystal structures were available from eubacteria (*Escherichia coli* and *Arthrobacter globiformis*), yeast (*Hansenula polymorpha* and *Pichia pastoris*), plants (*Pisum sativum*), and mammals (*Homo sapiens* and *Bos taurus*). All CAOs are homodimers consisting of subunits of ~700 residues[11] and share an archetypal CAO fold that was first described for the *E. coli* amine oxidase, ECAO.[12] ECAO is a four-domain protein that Parsons and colleagues aptly described as mushroom-shaped. An N-terminal "stalk" domain [domain 1 (D1)] is connected to the three remaining domains [domains 2−4 (D2−D4, respectively)] that constitute the "mushroom cap". D1 is unique to the ECAO structure and is proposed to exist in only three other CAOs from bacteria.[11] The cap of the mushroom is dominated by an ~450-residue C-terminal β-sandwich domain, D4, which houses the active site copper and TPQ. In addition to containing the active site, D4 contributes extensively to the dimer interface, packing against the same domain of the opposing subunit. The dimer is further stabilized by two β-hairpin "arms" that embrace the opposing subunit. The arms of each subunit interlock the dimer and, in the process, contribute approximately half of the protein surface buried in the dimer interface. The two remaining domains, D2 and D3, make up the periphery of the mushroom cap. These two domains share a high degree of structural homology and are suggested to be the result of a gene duplication event.[12]

CAOs are widespread in fungi, particularly in filamentous fungal species.[13] CAO studies in fungi have focused primarily on *Aspergillus niger*. The *A. niger* genome contains six CAO genes; the functional expression and characterization of three CAOs have been reported for two separate genes.[14,15] The filamentous fungi *Aspergillus nidulans* is a close relative of a number of industrial *Aspergilli* such as *A. niger*. Examination of the *A. nidulans* genome[13] indicates the presence of six uncharacterized CAOs and up to four MAOs. One gene (GenBank entry XP_663696) encodes a protein (AN6092.2) that is 36% identical in sequence to the so-called "lysyl oxidase" from *P. pastoris* (PPLO). The somewhat misleading name of this CAO is the result of observation that one of the two CAOs identified in *P. pastoris* was able to perform the in vitro oxidation of peptidyl lysine residues of synthetic elastin and collagen peptides.[16,17] However, the gene was subsequently cloned,[18] and the resulting gene product was shown unequivocally to contain TPQ but not LTQ.[19] In this work, we show that, similar to PPLO,[20] ANAO displays an apparent "lysyl oxidase-like" activity against tropoelastin to produce insoluble elastin masses as well as a modest cross-linking activity against α_{s1}-casein. Furthermore, in an attempt to explain ANAO's relatively broad substrate profile, the crystal structure of ANAO has been determined and refined to a resolution of 2.4 Å. The defining feature of the structure is a wide and accessible substrate channel, the dimensions of which give a clear explanation of how ANAO is able to oxidize such a variety of amine substrates. The structure of ANAO represents the first for a fungal CAO.

EXPERIMENTAL PROCEDURES

Cloning the Putative ANAO Gene. A codon-optimized synthetic gene sequence, based on the amino acid sequence (accession number Q5B038_EMENI in the EMBL data bank), was designed using an algorithm (as described in Patent WO/2006/077258[21]) for optimal expression in *A. niger*. The fragment was synthesized by DNA2.0 (http://www.dna20.com) and included the flanking restriction sites *Pac*I and *Asc*I. This fragment was digested with *Pac*I and *Asc*I and cloned between the *A. niger glaA* promoter and terminator sequences by exchanging with the *Pac*I−*Asc*I *phyA* fragment in pGBFIN-5 (in Patent WO 99/32617[22]), resulting in *A. niger* expression vector pGBFINZGR-1 (in Patent WO/2008/113799[23]).

Overexpression of ANAO in *A. niger*. Expression vector pGBFINZGR-1 was linearized by digestion with *Not*I, subsequently purified from *E. coli* vector sequences, and used to transform *A. niger* CBS513.88 (as described in refs 24 and 25). Single transformants containing multiple gene copies were isolated and purified, and spore preparations were made following standard techniques. The spore preparations were used as inocula for shake flask cultures containing the cultivation medium CSM-MES [150 g/L maltose, 6 g/L Soytone, 15 g/L $(NH_4)_2SO_4$, 1 g/L $NaH_2PO_4 \cdot H_2O$, 1 g/L $MgSO_4 \cdot 7H_2O$, 1 g/L L-arginine, 80 mg/L Tween 80, and 20 g/L MES (pH 6.2)]. Cultures were incubated at 34 °C. After 4−8 days, samples were centrifuged for 10 min at 5000*g* and supernatants were analyzed by sodium dodecyl sulfate−polyacrylamide gel electrophoresis (SDS−PAGE) for ANAO overexpression.

Purification of ANAO from *A. niger* Culture. Cell growth was disrupted after 5−6 days by the addition of 3.5 g/L sodium benzoate, followed by addition of 10 g/L $CaCl_2$ and 45 g/L Dicalite BF filter aid (Ghent, Belgium) after 6 h. Mycelium was removed by cloth filtration followed by additional filtration through Z-2000 and Z-200 filters (Pall, Mijdrecht, The Netherlands). Ultrafiltration was then conducted using an Amicon ultrafiltration cell (10 kDa molecular mass cutoff, Amicon, Millipore, Amsterdam, The Netherlands) until a 2−4-fold volume reduction was achieved.

The concentrated supernatant was equilibrated in 20 mM Tris (pH 7.5) to a conductivity of 1.8 mS/cm in an Amicon ultrafiltration cell. Subsequently, the sample was loaded onto a 5 mL Q-FF Hitrap Sepharose column (Pharmacia) using a flow rate of 5 mL/min and washed with 3 column volumes of 20 mM Tris (pH 7.5). Bound ANAO was eluted with a linear gradient from 20 mM Tris (pH 7.5) to 20 mM Tris (pH 7.5) containing 1 M NaCl. ANAO, identified using SDS−PAGE, eluted at ~340 mM NaCl. Fractions containing ANAO were pooled and transferred to an Amicon concentration cell (10 kDa molecular mass cutoff) to facilitate buffer exchange into 25 mM sodium phosphate (pH 6.6). The sample was then applied to a 5 mL Q-FF Hitrap Sepharose column pre-equilibrated with 25 mM sodium phosphate (pH 6.6). After being washed with 3 column volumes of 25 mM sodium phosphate (pH 6.6), bound ANAO was eluted using a 20-column volume linear gradient from 25 mM sodium phosphate (pH 6.6) to 25 mM sodium phosphate (pH 6.6) containing 1 M NaCl. Fractions containing ANAO were pooled, and the enzyme was deemed to be ~95% pure as determined by SDS−PAGE.

Enzyme Assays. A horseradish peroxidase (HRP) (Sigma Aldrich, St. Louis, MO)/2,2′-azinobis(3-ethyl)benzthiozoline-6-sulfonic acid (ABTS) (Fluka, Steinheim, Germany)-linked assay

was used to monitor the ANAO-induced oxidation of a lysine residue in the dipeptide Ac-Gly-Lys-OMe (Bachem, Bubendorf, Switzerland). This assay, first described for measuring MAO activity in tissue samples,[26] detects the hydrogen peroxide produced using HRP to catalyze the two-electron oxidation of chromogenic ABTS that was monitored spectrophotometrically (λ_{max} = 405 nm) using a Konelab analyzer Arena 30 (Thermo Scientific, Vantaa, Finland). Enzyme assays were conducted at 37 °C and pH 5.4.

Cross-linking reactions were performed on α-casein [a mixture of α_{S1}-casein and α_{S2}-casein (Sigma Aldrich, Zwijndrecht, The Netherlands)] using purified ANAO (~1.7 mg of enzyme/g of milk protein). The enzyme was added to 400 μL of 3% α-casein in 50 mM phosphate buffer (pH 7) and incubated for 16 h at 37 °C in a Thermomixer (Eppendorf, Hamburg, Germany). As a reference, heat-inactivated ANAO was used (15 min at 90 °C).

Cross-linking reactions were also performed with recombinant human tropoelastin isoform SHELΔ26A (synthetic human elastin without domain 26A) corresponding to amino acid residues 27−724 of GenBank entry AAC98394 (gi 182020).[27] Tropoelastin was dissolved in PBS [10 mM sodium phosphate and 150 mM NaCl (pH 7.4)] at a concentration of 10 mg/mL and mixed with 1 μM ANAO. The solution was incubated at 37 °C for 20 h and then cooled to 4 °C. The supernatant was retained for SDS−PAGE analysis, and the resulting cross-linked tropoelastin sheet was washed in PBS and water.

Characterization of ANAO-Cross-Linked α-Casein by Reversed Phase High-Performance Liquid Chromatography (RP-HPLC). Prior to analysis via RP-HPLC, milk samples were mixed with 3 volumes of a reducing buffer, containing Bis-Tris, urea, trisodium citrate, and dithiothreitol (DTT). The mixture was left at room temperature for 60 min, after which it was diluted further by the addition of 4 volumes of a urea solution adjusted to pH 2.5 with trifluoroacetic acid (TFA). Prior to application to the RP-HPLC column, samples were filtered through 0.22 μm filters. Analytical reversed phase chromatography (RP-HPLC) was conducted using two M 6000A pumps in combination with a high-sensitivity accessory block (Waters), an ISS-100 injector (Perkin-Elmer, Überlingen, Germany), a Waters model 680 gradient controller, and a Kratos 783 detector (Kratos Analytical, Ramsey, NJ). A 250 mm × 4.6 mm Widepore C18 column (Bio-Rad Laboratories, Richmond, CA) was used with a C18 cartridge (Bio-Rad) as a guard column. The column temperature was 30 °C. The equipment was linked to a data acquisition and processing system (Turbochrom, Perkin-Elmer). Solvent A was an acetonitrile/water/TFA acid (TFA) mixture (20:980:1, v/v/v), and solvent B contained the same components (900:100:0.8, v/v/v). The injection volume was 100 μL, and the absorbance of the eluent was monitored at 220 nm.

Characterization of ANAO-Cross-Linked Tropoelastin by Mass Spectrometry. Enzymatic proteolysis was performed using proteomics grade trypsin (Sigma, Steinheim, Germany). ANAO-cross-linked tropoelastin was dissolved at a concentration of 1 mg/mL in 50 mM Tris (pH 7.5) containing 0.02% NaN_3. The digestion was performed for 24 h at 37 °C at an enzyme: substrate ratio of 1:100 (w/w). MALDI-TOF/TOF experiments were performed using a system consisting of an Ultimate 3000 nanoHPLC system (Dionex, Idstein, Germany) and an Ultraflex III MALDI-TOF/TOF-MS system (Bruker Daltonik, Bremen, Germany) as described previously.[28] All fragment ion peak lists were submitted to a local mascot server (version 2.2.1; Matrix Science, London, U.K.).[29]

In another experiment, ANAO-cross-linked tropoelastin was totally hydrolyzed at a concentration of 1 mg/mL in 6 M HCl at 110 °C for 24 h. Desmosine was purchased from Elastin Products Co. (Owensville, MO) and dissolved in deionized water at a concentration of 10 μg/mL as a reference. The samples were evaporated to dryness using a SpeedVac and derivatized by propionylation. For propionylation, 100 μL of 0.1 N NH_4HCO_3 and 100 μL of a solution of 2-propanol containing 23% (v/v) propionic anhydride and 9% (v/v) NH_4OH were added to the samples. After reaction for 1 h, the samples were dried using a SpeedVac and redissolved in 50% (v/v) acetonitrile. Tandem MS experiments were conducted on a 4800 MALDI-TOF/TOF analyzer mass spectrometer (AB Sciex, Darmstadt, Germany) equipped with a Nd:YAG laser with a repetition rate of 200 Hz. One microliter of sample was mixed with 9 μL of a solution of 10 mg/mL α-cyano-4-hydroxycinnamic acid in an acetonitrile/0.1% TFA mixture (1:1, v/v), and 0.5 μL of the resulting mixture was spotted onto the sample plate and allowed to dry at room temperature.

Scanning Electron Microscopy. Scanning electron micrographs of cross-linked tropoelastin were obtained using a Philips (Eindhoven, The Netherlands) XL30 microscope at 15 kV. Insoluble cross-linked tropoelastin was air-dried on Thermanox plastic coverslips, which were then mounted onto aluminum stubs using conductive carbon paint and sputter coated with a 10 nm gold layer prior to analysis.

Crystallization and X-ray Data Collection. Prior to crystallization trials, the purified enzyme was dialyzed (10 kDa molecular mass cutoff, Amicon) against 3 × 500 mL changes of 50 mM HEPES (pH 7.2) with 150 mM KCl at 4 °C and concentrated to ~10 mg/mL. Initial vapor diffusion hanging drop crystallization trials were set up using a Mosquito robot (Molecular Dimensions Inc.) to dispense drops consisting of 150 nL of the protein solution and 150 nL of the reservoir solution over a reservoir of 75 μL at 20 °C. Crystalline material was observed under a number of conditions. An initial seed stock was made from crystals in 0.2 M $(NH_4)_2SO_4$ and 0.1 M sodium acetate (pH 4.9) with 30% (w/v) PEG 2000 MME from the NeXtal Classics screen (Qiagen). Crystal growth optimization around the initial conditions was manually performed using hanging drop vapor diffusion experiments consisting of 2 μL each of protein and reservoir solutions combined with streak seeking, yielding larger crystals after approximately 1 week. These crystals displayed poor diffraction of X-rays and were instead used to produce a second generation of seed stock. These new seeds were used in a subsequent round of crystal optimization in similar crystallization experiments (using identical crystallization conditions) used previously using streak seeding. A crystal grown in 0.2 M $(NH_4)_2SO_4$ and 0.1 M sodium acetate (pH 4.4) with 25% (w/v) PEG 2000 MME, once cryoprotected with 20% 2-methyl-2,4-pentanediol, gave reasonable diffraction to 2.4 Å resolution. In-house diffraction data were recorded on a Mar345 image plate (Marresearch) using Cu Kα X-rays produced by a Rigaku RU200H rotating anode generator using Osmic optics (both from Rigaku).

Structure Solution and Refinement. In-house diffraction data were integrated using MOSFLM,[30] the Laue group confidence and most probable space group determined using POINTLESS,[31] and intensities scaled together using SCALA.[31] Scaling of the data gave a large value for R_{merge} (25.4%) due largely to weak reflections past ~3.5 Å. However, the precision-indicating merging R factor, R_{pim}, gave a much more reasonable value of 9.7% with an $\langle I\rangle/\sigma(\langle I\rangle)$ in the outermost shell of 2.3. Data

collection at a synchrotron source gave little to no improvement in diffraction quality, indicating that it is crystal quality (mosaicity) that limits diffraction from this crystal form of ANAO. A search model for molecular replacement was generated (using CHAINSAW within CCP4[31]) using the PPLO model (33.5% sequence identity, Protein Data Bank entry 1w7c[32]) as a template with solvent and metal ligands removed and side chains pruned to a common atom based on a sequence alignment from ClustalW.[33] One molecule in the asymmetric unit gives a Matthews coefficient of 3.25 Å^3/Da corresponding to ~63% solvent. Molecular replacement using MOLREP[34] gave a solution for the data in space group *I*422 with one molecule in the asymmetric unit. The resulting model was first refined as a rigid body followed by multiple rounds of restrained refinement with REFMAC5,[35] interspersed with manual model correction against σA-weighted electron density maps in Coot.[36] During the early stages of refinement, a large proportion of the model was removed to minimize the substantial amount of model bias resulting from the molecular replacement solution. Loop regions were initially poorly defined in the density, and as a result, many sections of the model were obviously out of register with respect to the amino acid sequence. These regions were initially built as polyalanine until landmarks in the density, usually bulky side chains of aromatics, gave a good indication of the correct sequence register. Once the protein portion of the model was complete, water molecules were included either automatically or manually in Coot, based on reasonable electron density (with a $2F_o - F_c$ threshold of greater than 1σ), correct stereochemistry, and a reasonable *B* factor compared to those of surrounding atoms. N-Linked carbohydrate was well resolved in the electron density at five of the 11 putative glycosylation sites (belonging to the Asn-X-Thr/Ser sequon, where X can be any residue) and modeled as the appropriate glycans during refinement. The highest difference electron density peaks corresponded to the positions of the active site copper and secondary cation binding sites occupied by calcium ions. The TPQ was modeled into unbiased omit density during the final stages of refinement to reduce the bias of its orientation. The quality of the model was regularly checked for steric clashes, incorrect stereochemistry, poor side chain rotamers, and Ramachandran outliers using the MOLPROBITY server[37] and the validation tools within Coot.[36]

RESULTS

Cloning, Expression, and Functional Characterization of ANAO. A sequence comparison of CAOs revealed a region of only 29 residues that were highly conserved, and a motif was proposed that is useful in the identification of CAOs from fungi. Using this motif, I-H-D-[NS]-L-S-G-S-M-H-D-H-V-[IL]-N-F-K, a putative CAO gene sequence was identified in *A. nidulans*.[21] A codon-optimized version of this gene was synthesized and cloned in expression vector pGBFINZGR-1. The recombinant enzyme was overexpressed in *A. niger* and purified using ion exchange chromatography. Purified ANAO was estimated to be >95% homogeneous by SDS−PAGE.

The enzyme activity (expressed in units per milligram) was defined as the amount of H_2O_2 generated per minute at 37 °C and pH 5.4. The activity of recombinant ANAO, formulated in 50% glycerol, was assessed as ~2.8 units/mg of purified enzyme.

Cross-Linking α-Casein. Several food protein substrates [plant and bovine milk (results not shown)] were assayed for cross-linking using purified ANAO. Specifically, α-casein (a mixture of α_{S1}- and α_{S2}-casein) gave indications of cross-linking action as evidenced by SDS−PAGE (Figure 1A). Heptamers of α-casein were visible (approximately 210 kDa), indicating that at least one lysine of each casein monomer was modified leading to covalently linked oligomers. Oligomerization of α-casein was further proven by HPLC (Figure 1B); in the HPLC trace of the ANAO-treated α-casein, the α_{S1}-casein peak broadens and shifts to higher retention times, whereas most of the α_{S2}-casein peak stays intact. Moreover, at higher retention times, a further broad peak can be seen, indicative of cross-linking.

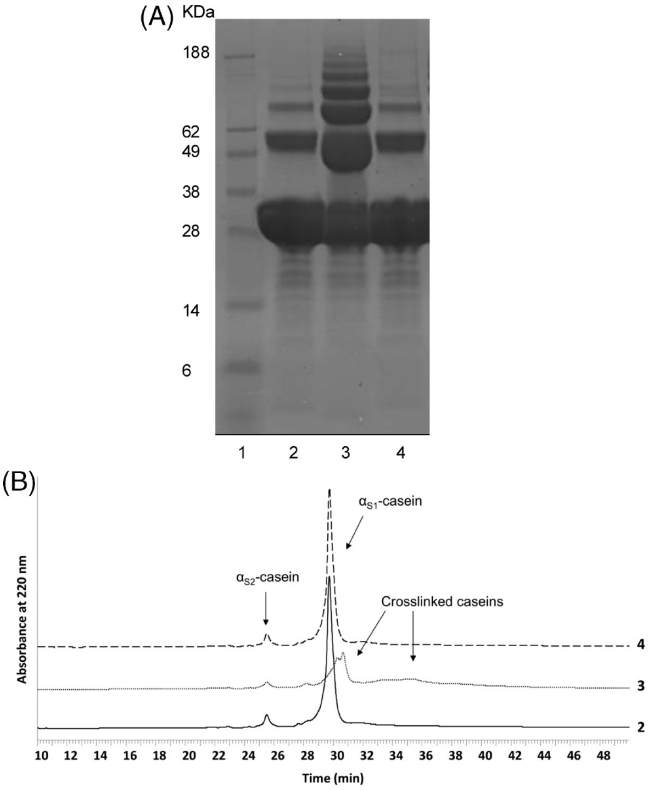

Figure 1. (A) SDS−PAGE gel showing cross-linking of α_{S1}-casein (~28 kDa): lane 1, Marker SeeBlue2 Plus; lane 2, α-casein; lane 3, α-casein treated with ANAO; lane 4, α-casein treated with inactivated ANAO. (B) Chromatograms from the same samples determined by HPLC.

Tropoelastin Cross-Linking. ANAO effectively cross-linked human tropoelastin into an insoluble elastic mass. SDS−PAGE analysis (Figure 2A) of the supernatant after the cross-linking reaction showed complete removal of monomer tropoelastin from a 10 mg/mL solution in the presence of 1 μM ANAO. Substantial removal of monomer in the presence of 0.1 μM ANAO, with the formation of dimer and trimer tropoelastin species, was also seen (data not shown). The resulting elastin sheet (Figure 2B) was a hydrogel and displayed stimulus responsive characteristics toward temperature and salt concentrations typical of cross-linked tropoelastin constructs.[38] Scanning electron microscopy (SEM) images of ANAO cross-linked tropoelastin (Figure 3) revealed a three-dimensional structure formed from coalesced spherules, which is an architecture regularly observed for insoluble elastin.[39]

Proteolysis experiments with trypsin revealed that ANAO-cross-linked tropoelastin, in contrast to mature elastin,[40] is

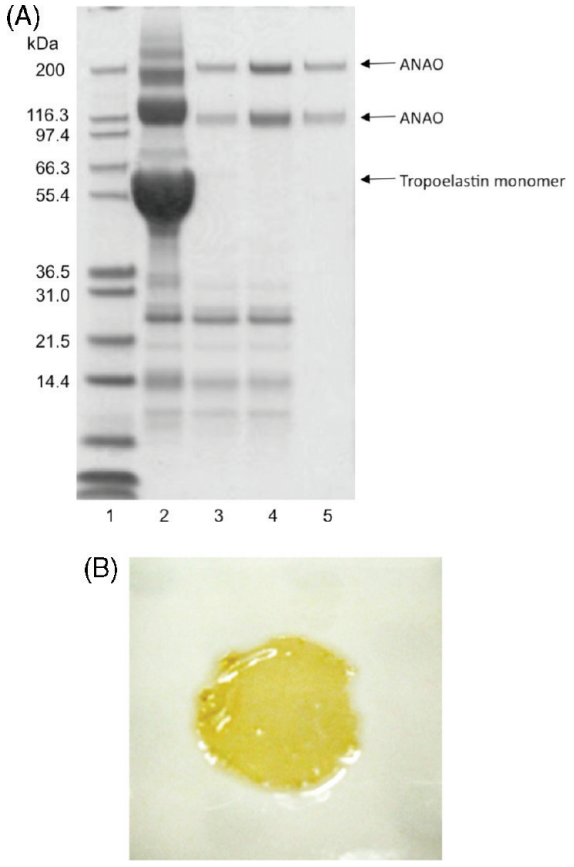

Figure 2. (A) SDS−PAGE gel showing removal of a large amount of tropoelastin monomer from solution following reaction with ANAO [40 μM ANAO dialyzed into 50 mM HEPES (pH 7) and 150 mM KCl (sample A, used for protein crystallization experiments) or 135 μM ANAO in 50% glycerol (pH 6.0) (sample B, used for enzymatic assays)]: lane 1, Mark 12 Standards; lane 2, 10 mg/mL tropoelastin; lane 3, 10 mg/mL tropoelastin with 1 μM ANAO (sample A) supernatant; lane 4, 10 mg/mL tropoelastin with 1 μM ANAO (sample B) supernatant; lane 5, 1 μM ANAO (sample A). The higher-molecular mass ANAO band most likely corresponds to unreduced disulfide bond-mediated homodimerization with the lower band corresponding to fully reduced ANAO monomer. (B) Insoluble ANAO-cross-linked tropoelastin sheet (1.2 cm diameter).

susceptible to cleavage by the protease. This indicates that the ANAO-cross-linked material is partially cross-linked, which is also supported by the fact that sequencing of the linear peptides from the enzymatic digest showed that unmodified lysines are present in the sample. However, MS analysis of the linear peptides from the digest also revealed the presence of oxidized deaminated lysines (Lys140, Lys315, and Lys717), so-called allysines, which are required for cross-linking of tropoelastin during in vivo elastogenesis. Indeed, tandem MS analysis of the totally hydrolyzed and propionylated samples showed that ANAO-cross-linked tropoelastin contains the tetrafunctional amino acid desmosine, which is formed upon condensation of three allysine residues and one lysine residue. The results confirm on the molecular level that oxidation of lysine residues by ANAO induces the formation of cross-linked amino acids that are unique to mature elastin.

Crystal Structure of ANAO. The structure of ANAO has been refined to a resolution of 2.45 Å with an $R_{overall}$ of 21.1% and an R_{free} of 25.4%. The data processing and refinement statistics are listed in Table 1. The model contains one molecule in the asymmetric unit, which consists of three conserved copper amine oxidase domains [D2−D4 (Figure 4A,B)] representing one-half of the biological homodimer. Overall, the structure of ANAO is most similar to that of PPLO with the two structures displaying an rmsd of ~1.4 Å for 676 C^{α} atoms (of 739 residues in chain A) when superposed using the secondary structure matching method (SSM[41]).

Residues 69−143 and 147−811 are resolved in the electron density and are included in our model. Similar to all structurally characterized CAOs, except ECAO, ANAO lacks domain D1. In ANAO, a short N-terminal strand (residues 69−82) prior to D2 is covalently linked to another short C-terminal strand via an intramolecular disulfide bridge between Cys72 and Cys779 in a similar fashion to that in PPLO.[20] The disulfides create a knot that effectively links the two subunits together. D2 consists of residues 83−199 and 200−332 form D3. D2 and D3 have the same topology and have roughly equal amounts of α-helix and β-sheet. A superposition, using SSM for the alignment, gives an rmsd of ~3.5 Å (for 71 C^{α} atoms). This similarity has led to the suggestion that D2 and D3 were likely to be a result of a gene duplication.[12] Residues 332−356 form a linker between the D3 and D4 domains crossing from one side of the structure to the other. This linker passes briefly through the symmetry-related D4 domain and effectively knots the two subunits together. Residues 357−774 comprise the largest domain, D4. Two central β-sheets constitute the largest portion of D4 and pack against the symmetry-related core of the other subunit. The active site topaquinone is located on the exterior side of a β-hairpin turn of the central β-sheet, positioning it at the bottom of the active site cavity. Three metal binding sites are also located on the peripheral edges of the central β-sheets of D4. Situated adjacent to the topaquinone is the active site Cu^{2+} ion binding site provided by three conserved histidine residues. Two secondary cation-binding sites are modeled as Ca^{2+} ions. Both Ca^{2+} sites are located close to the surface with one site slightly more solvent accessible than the other. In addition to a central β-sheet structure, D4 also comprises two protruding appendages: a single-β-hairpin "upper arm" (residues 569−602) and a two-β-hairpin "lower arm" (residues 476−489 and 756−773, respectively). These two arms embrace the other subunit and contribute extensively to the dimer interface, burying around 4700 $Å^2$ of the total solvent accessible dimer interface surface of 8790 $Å^2$ (calculated using PISA[42]). The dimer interface buries a large "inland lake" cavity that is characteristic of CAOs.[11] A secondary cavity connecting the active site and the lake (visible in Figure 5) has been proposed to provide a secondary route for small substrate molecular oxygen and products hydrogen peroxide and ammonia.[20,43] In ANAO, the lake is accessible to the exterior solvent via a small opening that is no more than 7.5 Å in diameter (measured between C^{β} atoms) between two symmetry-related phenylalanine residues (Phe613).

All structurally characterized CAOs contain charged residues or small-uncharged residues at the positions corresponding to Phe613 (Glu589 in PPLO, Lys572 in hDAO, Arg490 in AGAO, Ser517 in HPAO-1, Gly579 in BSAO, Gly580 in VAP-1, Gly500 in PSAO, and Asp581 in ECAO). In the case of ANAO, the presence of two large hydrophobic residues in such proximity at the entrance to the lake could potentially preclude the passage of charged species such as ammonia but would allow unhindered access to molecular oxygen. Conceivably, the presence of such a

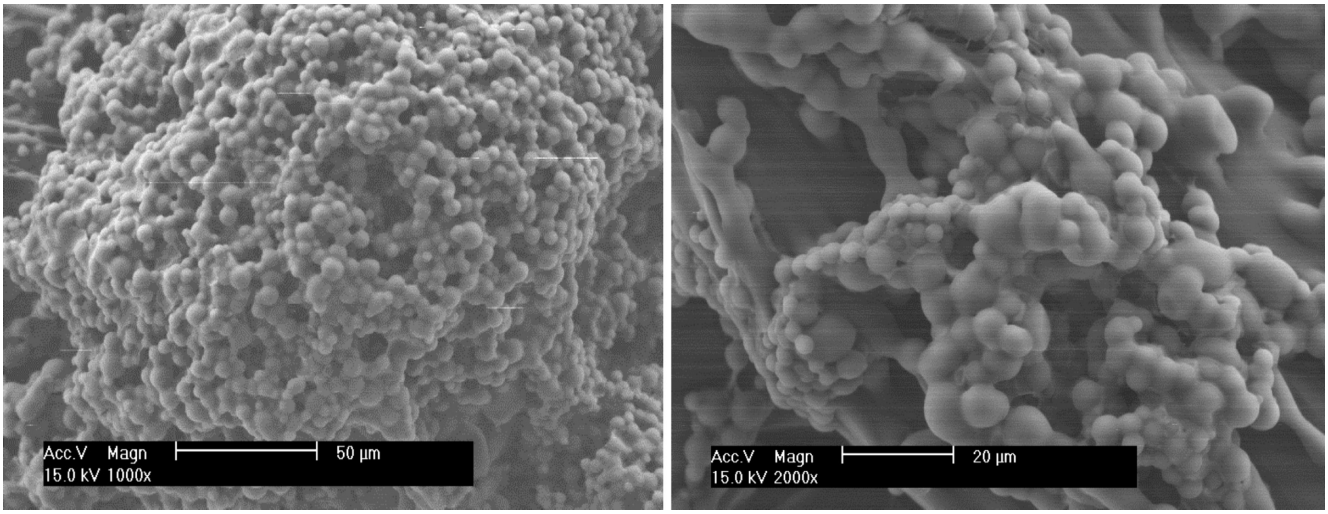

Figure 3. SEM analysis of insoluble elastin mass showed typical cross-linked elastin structure. Scale bars are indicated.

large active site cavity in ANAO reduces the need for a secondary passage to and from the active site.

Active Site of ANAO. Three conserved histidine residues bind the active site copper in CAOs. In ANAO, the copper is coordinated by $N^{\epsilon 2}$ of His552 and His554, $N^{\delta 1}$ of His718, and apically by a water molecule in a tetrahedral coordination geometry (Figure 4C). The TPQ cofactor is well-ordered in the productive "off-copper" conformation with O5 oriented toward the base of the substrate cavity, poised for reactivity with primary amine substrate (Figure 5). The off-copper conformation of the TPQ is stabilized by a hydrogen bonding interaction (Figure 4C) with a conserved Tyr residue (Tyr409 in ANAO). This tyrosine has previously been observed to stabilize a specific conformation of the substrate Schiff base formed during the catalytic mechanism to optimize α-proton abstraction by the conserved catalytic base, which in ANAO is Asp423.

There is a sufficient amount of contiguous residual $F_o - F_c$ density adjacent to the TPQ O5 position to suggest that at least a fraction of the TPQ was irreversibly inhibited, perhaps in a fashion similar to that of the TPQ—inhibitor complexes observed in various covalent inhibitor structures of CAOs.[44,45] The size and shape of this undescribed density is consistent with that of L-arginine, which was present in large quantities in the expression medium. Guanidinium compounds have long been known to inhibit some CAOs.[46] Attempts to confirm the size of the ligand using MALDI-TOF peptide mass fingerprinting experiments were unsuccessful, possibly because of the reactivity of the unprocessed TPQ with amino acid side chains during proteolytic digestion when preparing the sample for MS. Because of the ambiguity in confirming the identity of the inhibitor, and the relatively poor residual density, it has not been included in the final model.

Other Metal-Binding Sites. The structure of ANAO includes two secondary cation-binding sites that have been modeled as Ca^{2+} ions. These two sites are close to the surface of the protein (vide supra), with one site slightly more solvent accessible than the other. This shallower Ca^{2+} ion is coordinated by seven oxygen ligands provided by the carboxyl oxygen atoms of Glu604 (bidentate) and Glu701, a backbone carbonyl oxygen of Phe697, an amide carbonyl oxygen of Asn699, and two water molecules. The second calcium is ligated to three carboxyl group oxygen atoms provided by Asp561, Asp563, Asp707, the carbonyl backbone oxygen atoms of Phe562 and Leu708, and a water molecule. Both of these calcium sites are observed in all structurally characterized eukaryotic CAOs except *H. polymorpha* amine oxidase-1 (HPAO-1).[43]

Table 1. Diffraction Data and Refinement Statistics[a]

space group	*I*422
cell dimensions *a*, *b*, *c* (Å)	179.9, 179.9, 148.18
X-ray source	rotating anode
λ (Å)	1.5418
detector	MAR345
resolution range (Å)	40.22−2.43 (2.56−2.43)
no. of observed reflections	343580 (39160)
no. of unique reflections	44740 (5470)
completeness (%)	97.4 (82.5)
multiplicity	7.7 (7.2)
$\langle I\rangle/\sigma(\langle I\rangle)$	7.1 (2.3)
R_{merge}[b]	0.254 (0.815)
R_{pim}[c]	0.097 (0.322)
no. of reflections in working set	42466
no. of reflections in test set	2271
no. of protomers per asymmetric unit	1
total no. of atoms (non-H)	6368
no. of protein atoms	5908
no. of metal atoms	3
no. of water molecules	336
no. of carbohydrate residues	9
R_{cryst}	0.211 (0.315)
R_{free}	0.254 (0.360)
rmsd for bond lengths (Å)	0.007
rmsd for bond angles (deg)	1.05
$\langle B\rangle$ (Å^2)	21.3
Cruickshank's DPI[d]	0.32
PDB entry	3pgb

[a] Values in parentheses are for the highest-resolution shell. [b] $R_{merge} = \Sigma|I_h - \langle I_h\rangle|/\Sigma\langle I_h\rangle$. [c] $R_{pim} = \Sigma_{hkl}[1/(N-1)]^{1/2}\Sigma_i|I_i(hkl) - \langle I(hkl)\rangle|/\Sigma_{hkl}\Sigma_i I_i(hkl)$.[65] [d] Diffraction precision indicator as output from REFMAC5.[35]

dx.doi.org/10.1021/bi200555c |*Biochemistry* 2011, 50, 5718–5730

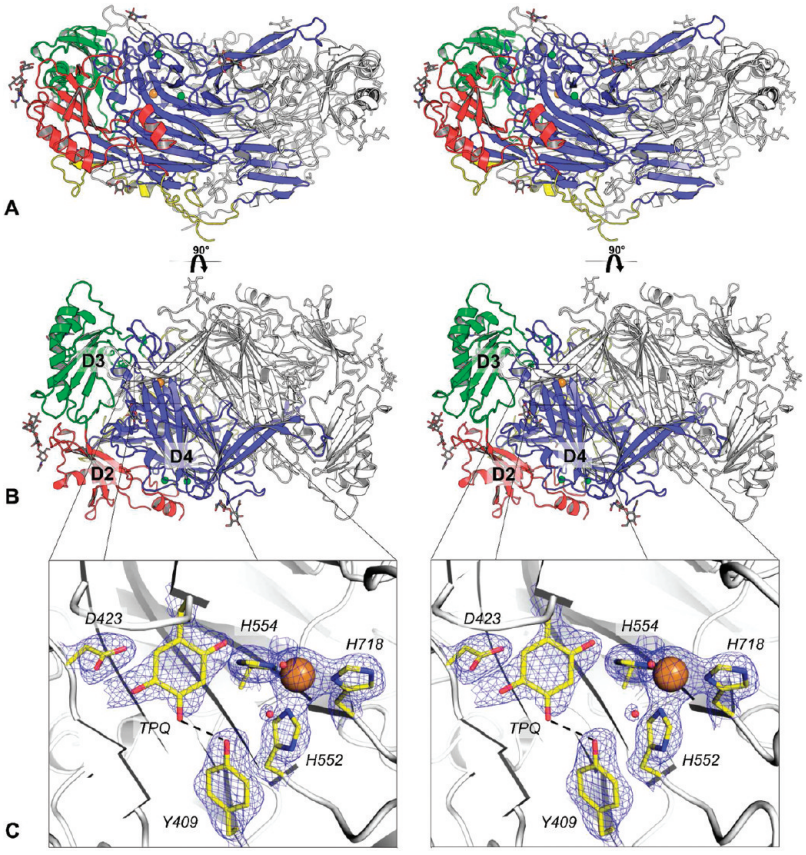

Figure 4. Stereoviews of the structure of ANAO in two orientations (A and B) with one subunit colored by CAO domains D2−D4. D2 is colored red, D3 green, and D4 blue. N- and C-terminal strands and a linker strand between D3 and D4 are colored yellow. Bound metals are shown as spheres with coppers colored orange and calcium ions colored green. Carbohydrates are shown as wheat-colored sticks. The symmetry-related subunit of the homodimer is colored white with associated metals and carbohydrates also colored white. A close-up of the catalytic site is shown in panel C with important residues shown as yellow sticks and the active site copper shown as an orange sphere. The associated electron density map for these features is shown as a $2F_o - F_c$ map contoured at 1.5σ.

Glycosylation Sites. ANAO expressed in *A. niger* is extensively glycosylated, with carbohydrate bound at five of the 11 putative N-linked glycosylation sites. In total, nine sugar residues are included in the model attached to Asn110 (NAG-NAG-MAN-MAN), Asn236 (NAG), Asn449 (NAG), Asn651 (NAG), and Asn704 (NAG-NAG). Although not sufficient for modeling, electron density suggests the presence of carbohydrate attached to Asn133, Asn228, and Asn776. Three other putative sites, Asn178, Asn568, and Asn588, show no obvious density to suggest the presence of glycosylation, although all three residues are well positioned on the surface of the molecule to be accessible by glycosyltransferases.

DISCUSSION

Biotechnological Implications of ANAO's Ability To Oxidise Lysine Residues on Casein and Tropoelastin. Protein often makes a major contribution in the texture of food products such as dairy, meat, and cereal products. Indeed, in food technology, there is an ongoing quest for modification of textures. Enzymatic cross-linking of proteins is an important example of such modification. Several examples of enzymes that induce protein cross-linking include the well-known and commercially available transglutaminase,[47,48] as well as tyrosinase[49,50] and laccase,[47,50] both of which are still at an experimental stage. A class not often mentioned to cross-link food protein is the CAOs. Some CAOs can modify the terminal ε-amino group of lysine residues within a protein, and the resulting allysine is a reactive group that in turn can react with another primary amine, or another allysine group, to form a covalent bond. PPLO has previously been demonstrated to cross-link tropoelastin, and in this study, we have demonstrated that ANAO is also proficient at catalyzing such a reaction.

Tropoelastin associates reversibly to form large multimer masses,[51] but these masses reversibly dissociate unless the interactions are stabilized by cross-linking.[52] Many studies focus on the use of chemical cross-linkers that stabilize associated tropoelastin to form elastin-based biomaterials in biomaterials applications.[53] Tropoelastin is an asymmetric, flexible molecule with 35 primary amines (namely, the ε-amino groups of lysyl residues) that are potentially amenable to cross-link formation.[51−55] Enzyme-based cross-linking of tropoelastin following the oxidation of lysines is an attractive alternative to chemical adduct formation as it approximates the natural process of elastin formation and has the potential to result in a material that more closely mimics the properties of natural elastin.[56]

We have also demonstrated that ANAO is capable of oxidizing lysines in α_{S1}-casein molecules. Bovine milk contains two major classes of protein: caseins and whey. Caseins are split into several subclasses (expressed as composition in skim milk in grams

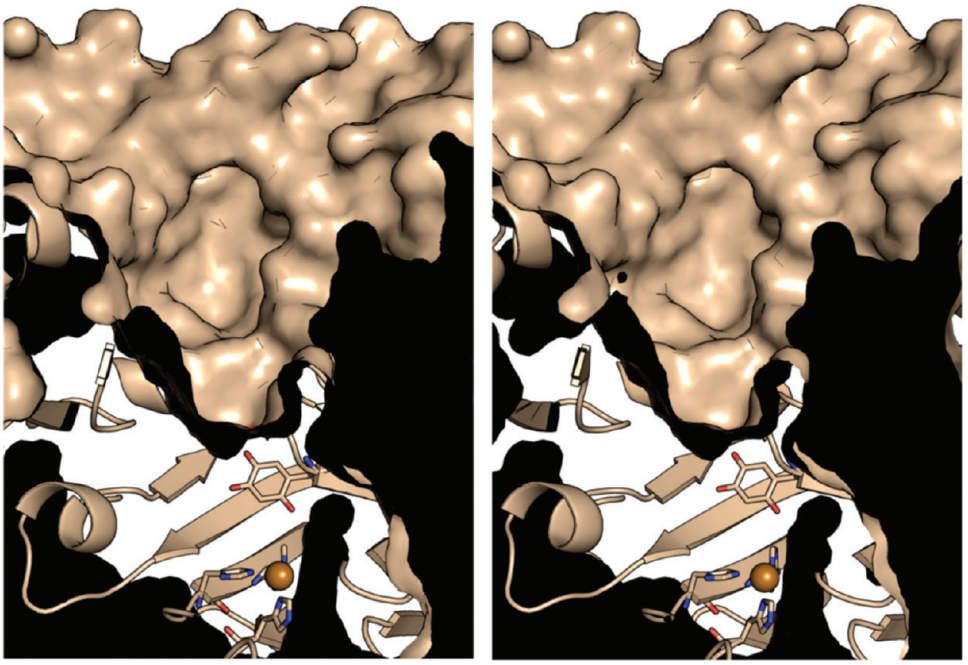

Figure 5. Cross-sectional stereoview of the substrate channel cavity leading to the catalytic site TPQ and Cu^{2+} ion. The TPQ- and copper-coordinating histidine residues are shown as sticks. The active site Cu^{2+} is shown as an orange sphere. A cross section of the secondary cavity leading to the catalytic site from the interior lake can be seen next to the copper ion.

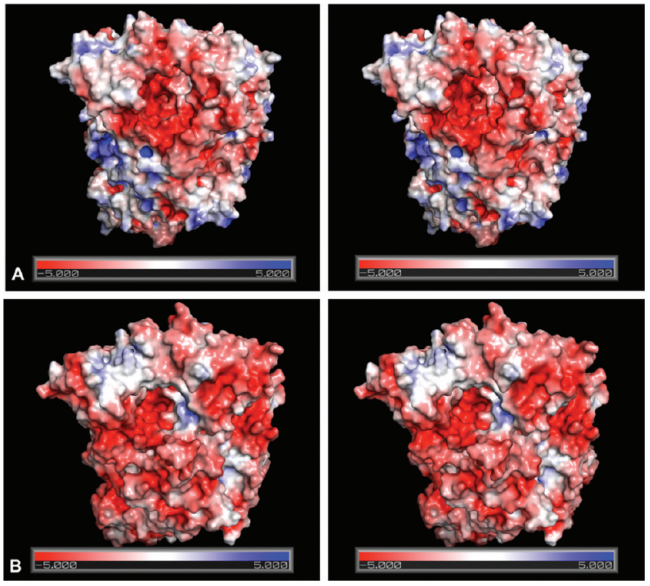

Figure 6. Stereoview of solvent accessible molecular surface representations of the ANAO (A) and PPLO (B) dimers colored by electrostatic potential at 0.15 M for −1 and +1 ion species at pH 7.0. Units are kT/e.

per liter): α_{S1} (12−15), α_{S2} (3−4), β (9−11), κ (2−4), and γ (1−2).[57] Caseins are not true globular proteins and have so far proven to be nonamenable to crystallization. As such, structural information has mostly been acquired via spectrophotometric techniques[58] and hints at why α_{S1}-casein is the only milk protein that can be modified by ANAO.[58,59] Taken together, these studies suggest that phosphoserines in α_{S1}-casein are situated in the middle part of the molecule (at positions 46 and 115) and, furthermore, that the middle of the molecule is bound by calcium phosphate bridges (inter- or intramolecular). Such a region would be expected to be inaccessible to an enzyme, such as ANAO, whereas the termini would be comparatively accessible. This also corroborates with the energy-minimized model for α_{S1}-casein.[59,60] α_{S1}-Casein has 14 lysines of 199 amino acids,[57] and three of these lysine residues (Lys3, Lys7, and Lys193) are located close to the peptide termini. Moreover, the N-terminus of α_{S1}-casein has a net positive charge at pH 6.6, with five of the first seven residues being positively charged, a unique feature within the group of milk proteins.[58,59] Correspondingly, the surface of the active site cavity of ANAO is predominately negative in charge (Figure 6), as would be expected for an enzyme that binds an amine substrate. Therefore, the N-terminus of α_{S1}-casein would be physically and chemically well suited to enter the active site of ANAO, where one or both of the N-terminal lysines could be reacted to form allysine. Once activated, these can react with other modified or unmodified lysines on α_{S1}-casein molecules, thereby forming covalent cross-links. Indeed, oligomers are observed in Figure 1A, and because most of the α_{S1}-casein peak in the HPLC trace disappears (in Figure 1B), it is likely that this fraction is modified. Most of the α_{S2}-casein peak is not altered, suggesting that this fraction is not modified even though it contains 24 lysines of 207 residues. One can conclude that these lysines are not accessible to the enzyme.

Substrate Channel and Comparison with the PPLO Channel. ANAO has a large and open substrate channel, which is clearly more accessible to substrate than that of other CAOs, with perhaps the exception of PPLO (Figure 7). A cross section of the ANAO active site channel shows that the cavity provides unimpeded access to the reactive quinone O5 of the TPQ (Figure 5). Upon comparison of CAO structures, three main features are proposed to modulate the accessibility of the substrate to the active site. The position of a helix across the lip of the active site cavity, for which we propose the name "lip helix", has a dramatic influence

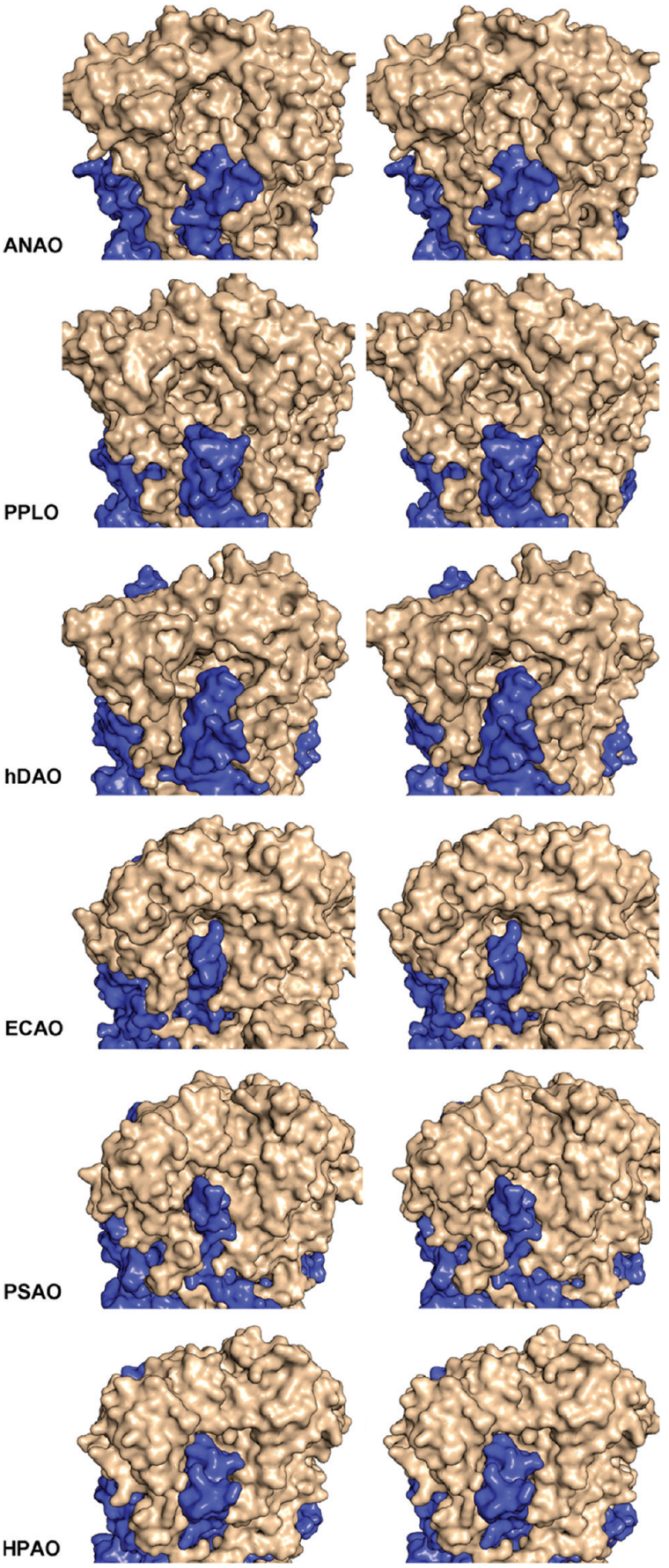

Figure 7. Continued

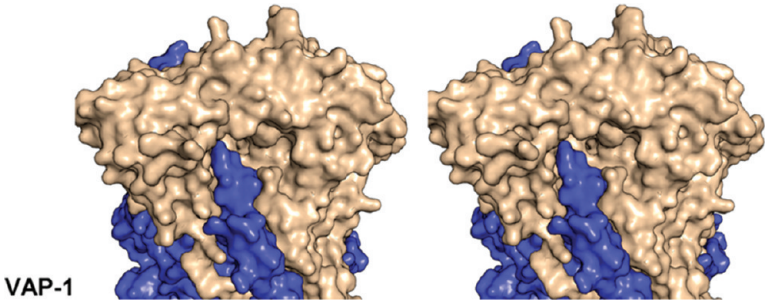

Figure 7. Stereoviews of the active site cavities of seven copper amine oxidases (ANAO, PPLO, hDAO, ECAO, PSAO, HPAO-1, and hVAP-1). The two subunits of the homodimers are colored wheat and blue to highlight the influence of the lower arm from the opposing subunit on defining the cavity dimensions.

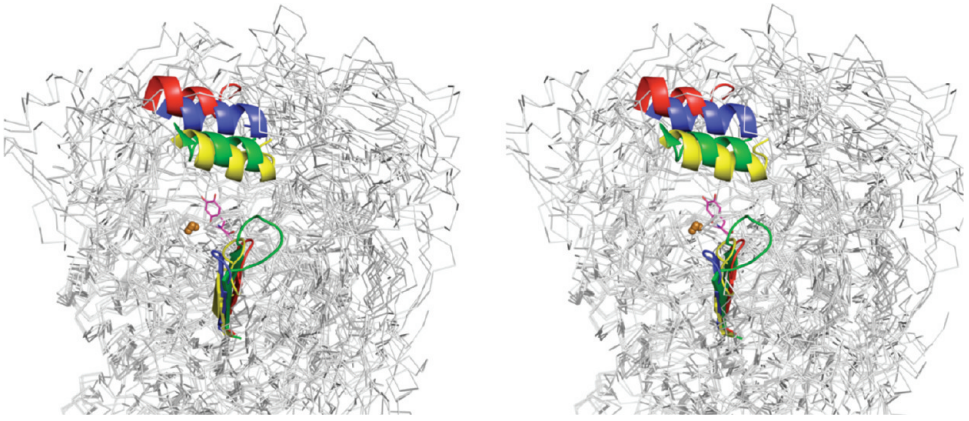

Figure 8. Overlay of four superposed copper amine oxidase structures shown as ribbons (white) in stereo. Two structural features (the lip helix and the β-hairpin lower arm) that define the dimensions of the substrate cavity are represented as cartoons in separate colors (ANAO in red, PPLO in blue, hDAO in green, and ECAO in yellow). The active site copper from each structure is shown as an orange sphere at the base of the active site channel, and the TPQ from ANAO (in the off-copper orientation) is shown as pink sticks. The structures were superposed using the secondary structure matching (SSM) method[41] and display the following rmsd values when compared with chain A of ANAO: 1.4 Å for PPLO (for 676 aligned C^{α} atoms), 2.3 Å for hDAO (for 623 aligned C^{α} atoms), and 2.1 Å for ECAO (for 529 aligned C^{α} atoms).

on the substrate channel dimensions (Figure 8). In ANAO, this lip helix is farther from the center of the cavity than that of any other CAO structure, being displaced by up to 2−3.5 Å at corresponding C^{α} positions of the lip helix in PPLO. When compared to those of other CAOs, this displacement is even more dramatic, with the lip helix limiting one side of the cavity by up to 15 Å in the case of ECAO when compared with ANAO. This displacement has a consequential effect on the position of a β-strand running antiparallel to the lip helix, which is located a short distance downstream (residues 238−245 in ANAO). This β-strand defines the dimensions of the waist of the cavity. The third feature influencing the accessibility of the substrate to the active site is the upper β-hairpin of the lower arm of the opposing dimer subunit. This β-hairpin is comprised of 13 residues in both ANAO and PPLO, shorter than that of any other CAO (Figure 7). Furthermore, the electrostatic surface potentials for both ANAO and PPLO (Figure 6) indicate that the active site of ANAO is even more negatively charged than PPLO.

A Word on Substrate Specificity in CAOs. Individual CAOs preferentially react with a defined subset of substrates to perform certain physiological roles. Structural studies have helped to elucidate some of the structural determinants of functionality in the CAO family of enzymes.[11] In each case, a unique architecture is observed in the region of the substrate channel. This variability appears to be one of the key mediators of substrate specificity. In humans, hDAO and hVAP-1 have different functions, and their substrate profiles are distinctly separate.[11,61,62] Although overall they share a high degree of similarity, there are some structural differences between them that can be reconciled with their substrate preference. Concurrent with a primary role in short diamine metabolism, the cavity in hDAO is narrow, and furthermore, the entrance of the substrate channel is divided into two parts. In comparison, the substrate cavity in hVAP-1 is wider, fitting with a proposed capacity to transiently bind lysine side chains projecting from lymphocyte cell surface proteins.[62] Using our work, this trend can be extended to include the unprecedentedly large and open active site cavity in ANAO that can accommodate and oxidize even larger substrates.

Substrate specificity in CAOs is further refined by the location of specific residues along the cavity wall. This theme has been explored previously in the structural comparisons of ECAO, AGAO, HPAO-1, and PSAO. In these structures, a conserved tyrosine residue "gates" access to the active site. Although evidence has been provided to suggest that this seems not to be the case in mammalian CAOs,[61] a similar gate role has been proposed for Leu469 in hVAP-1.[63,64]

Overall, the combination of large-scale observations such as comparative cavity size and subtle observations such as specific

residue identities allows us to propose a structural explanation for varying functionality. However, rationalizing the structural differences that give rise to functional variability in CAOs is not trivial, especially given the multiplicity of factors governing the recognition of a broad range of substrates.

CONCLUSIONS

ANAO is an extensively glycosylated enzyme that shares the archetypal CAO fold. Structurally, ANAO is most similar to PPLO, and a key feature of both structures is the presence of a large substrate channel. The dimensions of the cavity in ANAO presumably allow unhindered access to the active site for a range of primary amine substrates, including tropoelastin and α_{S1}-casein. The structure clearly demonstrates that the substrate channel is the structural determinant for the broad substrate specificity of the enzymes. The structure of ANAO provides a prime example of how the substrate cavity dimensions of CAOs help modulate substrate specificity. Tropoelastin is a natural substrate of LOX, an LTQ-containing copper amine oxidase that remains structurally uncharacterized. It is tempting to speculate that the topology of the substrate channel in LOX is similar to that of the functionally related ANAO. The physiological role and preferred in vivo substrate of ANAO in *A. nidulans*, however, remain unclear and require further investigation.

Accession Codes

The atomic coordinates and associated structure factors have been deposited in the Protein Data Bank as entry 3pgb.

AUTHOR INFORMATION

Corresponding Author

*E-mail: mitchell.guss@sydney.edu.au. Telephone: +61-2-9351-4302. Fax: +61 2 9351 5858.

Present Addresses

[||]Structural Biology Program, Centenary Institute, Sydney, NSW 2042, Australia.

Funding Sources

This research was supported by grants from the Australian Research Council (LP0669658 to C.A.C. and J.M.G. and DP1096608 to A.S.W.). A.P.M. was supported by an Australian Postgraduate Award for Industry. A.H. gratefully acknowledges financial support by the DFG (HE 6190/1-1).

ACKNOWLEDGMENT

We thank Anneke Remmerswaal and Jeroen Godefrooij for technical assistance and Jan-Metske van der Laan and Peter Dekker for critically reviewing the manuscript (all DSM Biotechnology Center). We thank Thom Huppertz of NIZO Food Research (Ede, The Netherlands) for performing HPLC. We also thank Ben Crossett (Sydney University Proteome Research Unit) for performing MALDI-TOF peptide mass fingerprinting experiments on purified ANAO.

DEDICATION

This paper is dedicated to the memory of Alard van Dijk who began the research on this enzyme but suddenly passed away before he could see these results.

ABBREVIATIONS

AGAO, *Ar. globiformis* amine oxidase; ANAO, *A. nidulans* amine oxidase; BSAO, bovine serum amine oxidase; CAO, copper-containing amine oxidase; CCP4, Collaborative Computational Project Number 4; hDAO, human diamine oxidase; ECAO, *E. coli* amine oxidase; HPAO-1, *H. polymorpha* amine oxidase; LOX, (mammalian) lysyl oxidase; LTQ, lysyl-tyrosyl quinone; MAN, mannose; MAO, monoamine oxidase; NAG, *N*-acetylglucosamine; PEG, polyethylene glycol; PPLO, *P. pastoris* amine oxidase; rmsd, root-mean-square deviation; SSM, secondary structure matching method; TPQ, 2,4,5-trihydroxyphenylalanine quinone; hVAP-1, human vascular adhesion protein-1.

REFERENCES

(1) Binda, C., Mattevi, A., and Edmondson, D. E. (2002) Structure-function relationships in flavoenzyme-dependent amine oxidations: A comparison of polyamine oxidase and monoamine oxidase. *J. Biol. Chem. 277*, 23973–23976.

(2) Bollinger, R. A., Brown, D. E., and Dooley, D. M. (2005) The formation of lysine tyrosylquinone (LTQ) is a self-processing reaction. Expression and characterization of a *Drosophila* lysyl oxidase. *Biochemistry 44*, 11708–11714.

(3) Ruggiero, C. E., and Dooley, D. M. (1999) Stoichiometry of the topa quinone biogenesis reaction in copper amine oxidases. *Biochemistry 38*, 2892–2898.

(4) Wang, S. X., Mure, M., Medzihradszky, K. F., Burlingame, A. L., Brown, D. E., and Dooley, D. M., et al. (1996) A crosslinked cofactor in lysyl oxidase: Redox function for amino acid side chains. *Science 273*, 1078–1084.

(5) Kagan, H. M., and Li, W. (2003) Lysyl oxidase: Properties, specificity, and biological roles inside and outside of the cell. *J. Cell. Biochem. 88*, 660–672.

(6) Lucero, H. A., and Kagan, H. M. (2006) Lysyl oxidase: An oxidative enzyme and effector of cell function. *Cell. Mol. Life Sci. 63*, 2304–2316.

(7) Smith-Mungo, L. I., and Kagan, H. M. (1998) Lysyl oxidase: Properties, regulation and multiple functions in biology. *Matrix Biol. 16*, 387–398.

(8) Boyce, S., Tipton, K. F., O'Sullivan, M. I., Davey, G. P., Motherway Gildea, M., McDonald, A. G., et al. (2009) in *Copper Amine Oxidases* (Floris, G., and Mondovi, B., Eds.) pp 5−17, Taylor and Francis, Boca Raton, FL.

(9) Schwelberger, H. G. (2004) in *Histamine: Biology and Medical Aspects* (Falus, A., Ed.) pp 43−52, SpringMed Publishing, Budapest.

(10) O'Sullivan, J., Unzeta, M., Healy, J., O'Sullivan, M. I., Davey, G., and Tipton, K. F. (2004) Semicarbazide-sensitive amine oxidases: Enzymes with quite a lot to do. *Neurotoxicology 25*, 303–315.

(11) Guss, J. M., Zanotti, G., and Salminen, T. (2009) in *Copper Amine Oxidases: Structures, Catalytic Mechanisms and Role in Pathophysiology* (Floris, G., and Mondovi, B., Eds.) pp 119−141, Taylor and Francis, Boca Raton, FL.

(12) Parsons, M. R., Convery, M. A., Wilmot, C. M., Yadav, K. D., Blakeley, V., and Corner, A. S., et al. (1995) Crystal structure of a quinoenzyme: Copper amine oxidase of *Escherichia coli* at 2 Å resolution. *Structure 3*, 1171–1184.

(13) Galagan, J. E., Calvo, S. E., Cuomo, C., Ma, L. J., Wortman, J. R., and Batzoglou, S., et al. (2005) Sequencing of *Aspergillus nidulans* and comparative analysis with *A. fumigatus* and *A. oryzae*. *Nature 438*, 1105–1115.

(14) Frebort, I., Tamaki, H., Ishida, H., Pec, P., Luhova, L., and Tsuno, H., et al. (1996) Two distinct quinoprotein amine oxidases are induced by n-butylamine in the mycelia of *Aspergillus niger* AKU 3302. Purification, characterization, cDNA cloning and sequencing. *Eur. J. Biochem. 237*, 255–265.

(15) Frebort, I., Matsushita, K., Toyama, H., Lemr, K., Yamada, M., and Adachi, O. (1999) Purification and characterization of methylamine oxidase induced in *Aspergillus niger* AKU 3302. *Biosci., Biotechnol., Biochem. 63*, 125–134.

(16) Green, J., Haywood, G. W., and Large, P. J. (1983) Serological differences between the multiple amine oxidases of yeasts and comparison of the specificities of the purified enzymes from *Candida utilis* and *Pichia pastoris*. *Biochem. J. 211*, 481–493.

(17) Tur, S. S., and Lerch, K. (1988) Unprecedented lysyloxidase activity of *Pichia pastoris* benzylamine oxidase. *FEBS Lett. 238*, 74–76.

(18) Kuchar, J. A., and Dooley, D. M. (2001) Cloning, sequence analysis, and characterization of the 'lysyl oxidase' from *Pichia pastoris*. *J. Inorg. Biochem. 83*, 193–204.

(19) Dove, J. E., Smith, A. J., Kuchar, J., Brown, D. E., Dooley, D. M., and Klinman, J. P. (1996) Identification of the quinone cofactor in a lysyl oxidase from Pichia pastoris. *FEBS Lett. 398*, 231–234.

(20) Duff, A. P., Cohen, A. E., Ellis, P. J., Kuchar, J. A., Langley, D. B., and Shepard, E. M., et al. (2003) The crystal structure of *Pichia pastoris* lysyl oxidase. *Biochemistry 42*, 15148–15157.

(21) Roubos, J. A., Donkers, S. P., Stam, H., and Van Peij, N. N. M. E. (2006) International Patent WO/2006/077258.

(22) van Den Brink, J. M., Selten, G. C. M., and Van Den Homberg, J. P. T. W. (1999) U.S. Patent WO 99/32617.

(23) van Dijk, A. A., Dekker, P. J. T., Westerlaken, I., and Bakhuis, J. G. (2008) International Patent WO/2008/113799.

(24) Tilburn, J., Scazzocchio, C., Taylor, G. G., Zabicky-Zissman, J. H., Lockington, R. A., and Davies, R. W. (1983) Transformation by integration in *Aspergillus nidulans*. *Gene 26*, 205–221.

(25) Kelly, J. M., and Hynes, M. J. (1985) Transformation of *Aspergillus niger* by the amdS gene of *Aspergillus nidulans*. *EMBO J. 4*, 475–479.

(26) Szutowicz, A., Kobes, R. D., and Orsulak, P. J. (1984) Colorimetric Assay for Monoamine-Oxidase in Tissues Using Peroxidase and 2,2′-Azinodi(3-Ethylbenzthiazoline-6-Sulfonic Acid) as Chromogen. *Anal. Biochem. 138*, 86–94.

(27) Wu, W. J., Vrhovski, B., and Weiss, A. S. (1999) Glycosaminoglycans mediate the coacervation of human tropoelastin through dominant charge interactions involving lysine side chains. *J. Biol. Chem. 274*, 21719–21724.

(28) Heinz, A., Jung, M. C., Duca, L., Sippl, W., Taddese, S., and Ihling, C., et al. (2010) Degradation of tropoelastin by matrix metalloproteinases: Cleavage site specificities and release of matrikines. *FEBS J. 277*, 1939–1956.

(29) Perkins, D. N., Pappin, D. J. C., Creasy, D. M., and Cottrell, J. S. (1999) Probability-based protein identification by searching sequence databases using mass spectrometry data. *Electrophoresis 20*, 3551–3567.

(30) Leslie, A. G. W. (1992) Recent changes to the MOSFLM package for processing film and image plate data. *Joint CCP4 and ESF-EAMCB Newsletter on Protein Crystallography*, Vol. 26.

(31) Collaborative Computational Project Numer 4. (1994) The CCP4 suite: Programs for protein crystallography. *Acta Crystallogr. D50*, 760–763.

(32) Duff, A. P., Cohen, A. E., Ellis, P. J., Hilmer, K., Langley, D. B., and Dooley, D. M., et al. (2006) The 1.23 Angstrom structure of *Pichia pastoris* lysyl oxidase reveals a lysine-lysine cross-link. *Acta Crystallogr. D62*, 1073–1084.

(33) Larkin, M. A., Blackshields, G., Brown, N. P., Chenna, R., McGettigan, P. A., and McWilliam, H., et al. (2007) Clustal W and Clustal X version 2.0. *Bioinformatics 23*, 2947–2948.

(34) Vagin, A., and Teplyakov, A. (2010) Molecular replacement with MOLREP. *Acta Crystallogr. D66*, 22–25.

(35) Murshudov, G. N., Vagin, A. A., and Dodson, E. J. (1997) Refinement of macromolecular structures by the maximum-likelihood method. *Acta Crystallogr. D53*, 240–255.

(36) Emsley, P., and Cowtan, K. (2004) Coot: Model-building tools for molecular graphics. *Acta Crystallogr. D60*, 2126–2132.

(37) Davis, I. W., Leaver-Fay, A., Chen, V. B., Block, J. N., Kapral, G. J., and Wang, X., et al. (2007) MolProbity: All-atom contacts and structure validation for proteins and nucleic acids. *Nucleic Acids Res. 35*, W375–W383.

(38) Mithieux, S. M., Rasko, J. E. J., and Weiss, A. S. (2004) Synthetic elastin hydrogels derived from massive elastic assemblies of self-organized human protein monomers. *Biomaterials 25*, 4921–4927.

(39) Mithieux, S. M., Tu, Y., Korkmaz, E., Braet, F., and Weiss, A. S. (2009) In situ polymerization of tropoelastin in the absence of chemical cross-linking. *Biomaterials 30*, 431–435.

(40) Werb, Z., Banda, M. J., McKerrow, J. H., and Sandhaus, R. A. (1982) Elastases and elastin degradation. *J. Invest. Dermatol. 79* (Suppl. 1), 154s–159s.

(41) Krissinel, E., and Henrick, K. (2004) Secondary-structure matching (SSM), a new tool for fast protein structure alignment in three dimensions. *Acta Crystallogr. D60*, 2256–2268.

(42) Krissinel, E., and Henrick, K. (2007) Inference of macromolecular assemblies from crystalline state. *J. Mol. Biol. 372*, 774–797.

(43) Li, R., Klinman, J. P., and Mathews, F. S. (1998) Copper amine oxidase from *Hansenula polymorpha*: The crystal structure determined at 2.4 Å resolution reveals the active conformation. *Structure 6*, 293–307.

(44) Langley, D. B., Trambaiolo, D. M., Duff, A. P., Dooley, D. M., Freeman, H. C., and Guss, J. M. (2008) Complexes of the copper-containing amine oxidase from *Arthrobacter globiformis* with the inhibitors benzylhydrazine and tranylcypromine. *Acta Crystallogr. F64*, 577–583.

(45) Wilmot, C. M., Murray, J. M., Alton, G., Parsons, M. R., Convery, M. A., and Blakeley, V., et al. (1997) Catalytic mechanism of the quinoenzyme amine oxidase from *Escherichia coli*: Exploring the reductive half-reaction. *Biochemistry 36*, 1608–1620.

(46) Bardsley, W. G., and Ashford, J. S. (1972) Inhibition of pig kidney diamine oxidase by substrate analogues. *Biochem. J. 128*, 253–263.

(47) Huppertz, T. (2009) *Novel applications of enzymes in the dairy sector: Optimizing functional properties of milk proteins by enzymatic cross-linking*, Woodhead Publishing, Cambridge, U.K.

(48) Santos, M., and Torne, J. M. (2009) Recent patents on transglutaminase production and applications: A brief review. *Recent Pat. Biotechnol. 3*, 166–174.

(49) Cura, D. E., Lille, M., Partanen, R., Kruus, K., Buchert, J., and Lantto, R. (2010) Effect of *Trichoderma reesei* tyrosinase on rheology and microstructure of acidified milk gels. *Int. Dairy J. 20*, 830–837.

(50) Cura, D. E., Lantto, R., Lille, M., Andberg, M., Kruus, K., and Buchert, J. (2009) Laccase-aided protein modification: Effects on the structural properties of acidified sodium caseinate gels. *Int. Dairy J. 19*, 737–745.

(51) Clarke, A. W., Arnspang, E. C., Mithieux, S. M., Korkmaz, E., Braet, F., and Weiss, A. S. (2006) Tropoelastin massively associates during coacervation to form quantized protein spheres. *Biochemistry 45*, 9989–9996.

(52) Muiznieks, L. D., Jensen, S. A., and Weiss, A. S. (2003) Structural changes and facilitated association of tropoelastin. *Arch. Biochem. Biophys. 410*, 317–323.

(53) Wise, S. G., and Weiss, A. S. (2009) Tropoelastin. *Int. J. Biochem. Cell Biol. 41*, 494–497.

(54) Baldock, C., Oberhauser, A. F., Lammie, D., Siegler, V., Mithieux, S. M., and Tu, Y., et al. (2011) Shape of tropoelastin, the hyper-extensible protein that controls human tissue elasticity. *Proc. Natl. Acad. Sci. U.S.A.*in press.

(55) Toonkool, P., Regan, D. G., Kuchel, P. W., Morris, M. B., and Weiss, A. S. (2001) Thermodynamic and hydrodynamic properties of human tropoelastin: Analytical ultracentrifuge and pulsed field-gradient spin-echo NMR studies. *J. Biol. Chem. 276*, 28042–28050.

(56) Clarke, A. W., Wise, S. G., Cain, S. A., Kielty, C. M., and Weiss, A. S. (2005) Coacervation is promoted by molecular interactions between the PF2 segment of fibrillin-1 and the domain 4 region of tropoelastin. *Biochemistry 44*, 10271–10281.

(57) Farrell, H. M., Jr., Jimenex-Flores, R., Bleck, G. T., Brown, E. M., Butler, J. E., and Creamer, L. K., et al. (2004) Nomenclature of the proteins of cow's milk: Sixth revision. *J. Dairy Sci. 87*, 1641–1674.

(58) Malin, E. L., Brown, E. M., Wickham, E. D., and Farrell, H. M., Jr. (2005) Contributions of terminal peptides to the associative behavior of α_{s1}-casein. *J. Dairy Sci. 88*, 2318–2328.

(59) Fox, P. F., and McSweeney, P. L. H. (1998) *Dairy Chemistry and Biochemistry*, Blackie, London.

(60) Kumosinski, T. F., Brown, E. M., and Farrell, H. M. (1991) 3-Dimensional Molecular Modeling of Bovine Caseins: α-S1-Casein. *J. Dairy Sci. 74*, 2889–2895.

(61) McGrath, A. P., Hilmer, K. M., Collyer, C. A., Shepard, E. M., Elmore, B. O., and Brown, D. E., et al. (2009) Structure and inhibition of human diamine oxidase. *Biochemistry 48*, 9810–9822.

(62) Salmi, M., Yegutkin, G. G., Lehvonen, R., Koskinen, K., Salminen, T., and Jalkanen, S. (2001) A cell surface amine oxidase directly controls lymphocyte migration. *Immunity 14*, 265–276.

(63) Jakobsson, E., Nilsson, J., Ogg, D., and Kleywegt, G. J. (2005) Structure of human semicarbazide-sensitive amine oxidase/vascular adhesion protein-1. *Acta Crystallogr. D61*, 1550–1562.

(64) Airenne, T. T., Nymalm, Y., Kidron, H., Smith, D. J., Pihlavisto, M., and Salmi, M., et al. (2005) Crystal structure of the human vascular adhesion protein-1: Unique structural features with functional implications. *Protein Sci. 14*, 1964–1974.

(65) Weiss, M. S. (2001) Global indicators of X-ray data quality. *J. Appl. Crystallogr. 34*, 130–135.